Implementation of Digitally Scanned P-OFDR using a Digital Coherent Transceiver

Fatima Al-Shaikhli[1], Maurice O'Sullivan[2], Charles Laperle[2], and Rongqing Hui[1]
1: Dept. of Electrical Engineering and Computer Science, University of Kansas, Lawrence, KS 66045 USA
2: Ciena Corporation, Ottawa, ON, K2K 0L1, Canada
Author email: Fatima.al-shaikhli@ku.edu

Abstract: We present a novel measurement technique for P-OFDR with a digitally created linear chirp in the transmitter and vector complex optical field detection to measure the Stokes parameters along the fiber.

1. Introduction

For transmission applications Rayleigh scattering is a major limiting factor for fiber loss reduction, whereas for sensing applications, Rayleigh scattering can be utilized to characterize parameters along the fiber [1]. Distributed fiber-optic sensing (DFOS) is useful for many applications ranging from telecommunication networks to military installations. DFOS is widely applied to continuously monitor the integrity of buildings, bridges, dams, and aircraft. Specialty fibers with enhanced backscattering were also developed to improve signal to noise ratio for DFOS [2]. Optical Time Domain Reflectometry (OTDR) and Optical Frequency Domain Reflectometry (OFDR) are two basic categories of DFOS. While OTDR uses short optical pulses, OFDR uses broadband optical spectrum through linear chirping or modulation to achieve high spatial resolution [3,4]. For many practical applications, external perturbations along a fiber cable, such as stress and strain, may introduce significant changes in the birefringence without changing the fiber loss. In such cases polarization-sensitive sensing would be most useful to measure the change of distributed birefringence along the fiber [3-9].

Polarization-Sensitive OFDR (P-OFDR) is typically implemented by linearly scanning the wavelength of a tunable laser (TL) over a wide window to achieve a fine spatial resolution, and the state of polarization (SOP) of the backscattered optical signal originated from different locations along the fiber is analyzed at the receiver. Although chirping rate and linearity of a TL can be calibrated through an additional optical interferometer, phase continuity of optical carrier cannot be guaranteed during wavelength tuning. Thus, optical intensity detection (either direct or coherent) is usually used after a polarization beam spitter (PBS) to determine the SOP of the optical signal [3,4,9].

In this paper we demonstrate a simplified P-OFDR based on a commercial digital coherent transceiver. In this implementation, linear optical frequency chirp is obtained directly through digital modulation which ensures linearity, repeatability, and optical phase continuity across the chirping bandwidth. A homodyne receiver with both phase-diversity and polarization diversity detects the vector complex field of the optical signal, so that the Stokes parameters of backscattered optical signal originated from different locations along the fiber can be fully characterized. A spatial resolution on the order of $10\ mm$ was obtained with an applied chirping bandwidth of $26\ GHz$.

2. Experiment and results

The block diagram of the experimental setup is shown in Fig 1, where a digital coherent transceiver (Ciena, WaveLogic-AI) is used. The real and imaginary parts of a linearly chirped waveform are applied on an in-phase/quadrature (I/Q) electrooptic modulator through digital-to-analog converters (DAC) (68GS/s sampling rate) and RF driving amplifiers. Carrier-suppressed optical single sideband modulation is used to linearly chirp the signal optical frequency from $4\ GHz$ to $30\ GHz$ within a $1538\ ns$ time window. A short section of low frequency noise within a 1.5 GHz bandwidth is also applied to help stabilize the modulator bias control. The time domain waveforms and the corresponding optical spectrum are shown in the insets (a), (b) and (c) in Fig 1. The optical signal generated from the transmitter (Tx) is split into two parts, 90% of it is used as the local oscillator (LO) for coherent detection and the other 10% is sent to the fiber under test (FUT) via an EDFA in which the signal is amplified to 13dBm, that is followed by an optical circulator. The FUT consists of ~17.5 m SMF-28 spliced with 20 m OFS high scattering fiber (HSF) which has approximately 10 dB higher Rayleigh scattering compared to SMF-28 [2]. The backscattered light from FUT is redirected by the circulator and amplified by another EDFA before detected by the receiver. A bandpass optical filter with $1\ nm$ bandwidth is used to eliminate broadband noise from the two EDFAs.

The coherent homodyne detection receiver, equipped with both polarization diversity and phase diversity, measures the I and Q components of both x and y polarizations and the differential phase between them, and thus, the Stokes parameters can be fully characterized. Because the LO has the same frequency chirp as the optical signal, de-chirping is performed in the coherent receiver [10]. The de-chirped waveforms (only the real and imaginary parts of the x-

component) and the corresponding complex spectra (for both x and y components) are shown in insets (d) and (e) of Fig.1. For a chirp rate of $\xi = \Delta F/T$, with $\Delta F = 26\ GHz$ the chirp bandwidth and $T = 1538\ ns$ the chirp length, the component at frequency f in the de-chirped RF spectrum corresponds to the contribution of backscattering from position $z = (f/\xi)(c/2n)$ along the FUT, where c is the speed of light, $n = 1.47$ is the refractive index of the fiber, and the factor 2 accounts for roundtrip propagation in the FUT. Note that this position z is a differential length between the LO and the point of backscattering along the FUT. Therefore, a ~75m fiber delay line is added to the LO path to compensate for the delay caused by the EDFAs and pigtails of optical components in the signal path. This moves the spectral component corresponding to the FUT input point to approximately $-1.5\ GHz$ in the spectrum.

To demonstrate the capability to identify the position where the stress is applied, we inserted an inline polarization controller (PC) (PLC-003, General Photonics) in the section of HFS which can introduce linear birefringence by squeezing and/or rotating the fiber.

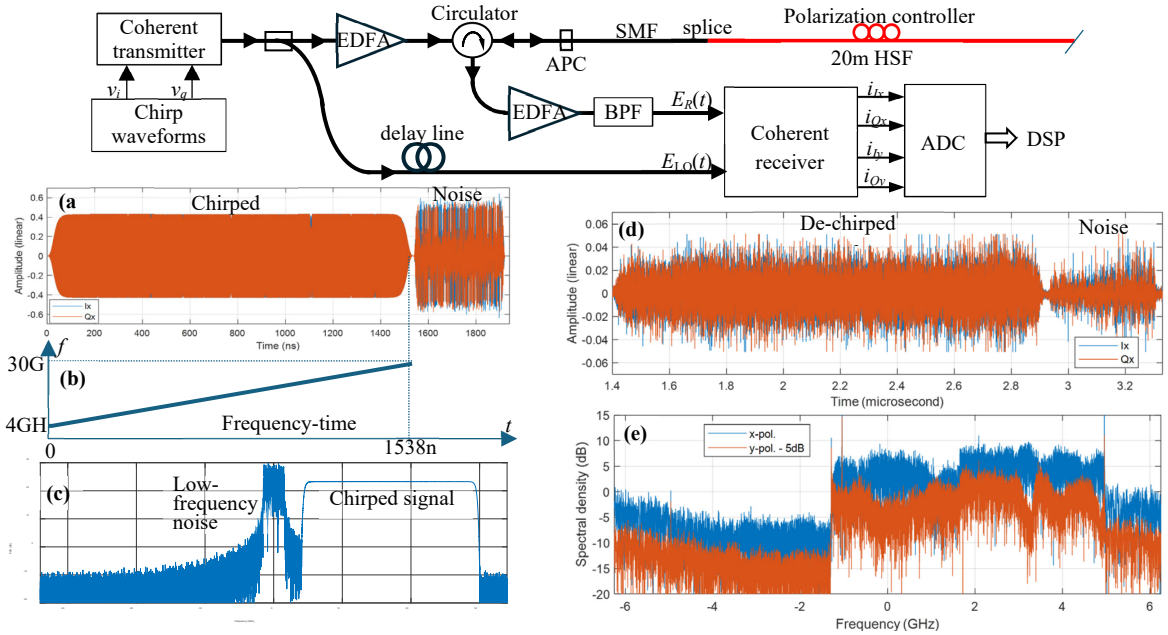

Fig 1. Experimental Setup. Insets: (a) real and imaginary parts of chirped waveform applied to modulator, (b) frequency-time diagram of linear chirp, (c) spectrum of optical signal, (d) real and imaginary parts of de-chirped waveforms (only x-component shown) at the receiver output, and (e) de-chirped complex spectra for the x and y-polarized components (y-component is reduced by 5dB for better display)

Note that in the inset (e) of Fig.1, the power spectral densities (PSD) above $-1.5\ GHz$ are originated from the backscattering of the FUT. The x and y- polarized components are complementary, indicating that the Rayleigh backscattered light maintains a high degree of polarization. The transition between SMF-28 and HSF is at 2.65 GHz. With a chirp rate of $\xi = 1.6905 \times 10^{16} Hz/s$, the conversion between frequency f and location z is $z = z_0 + 6.177 \times 10^{-9} f$, where z_0 is a constant determined by the differential delay between the LO and the input of the FUT.

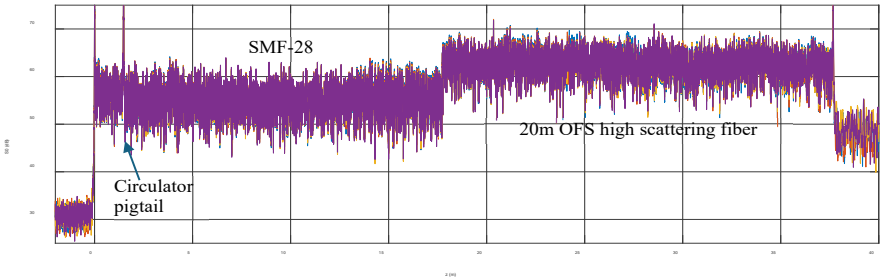

Fig 2. spectral density of the total power as the function scatter position z

Fig.2 shows measured spectral density of the total power which is equivalent to $S_0 = |E_x|^2 + |E_y|^2$ (E_x and E_y represent optical fields of x and y- polarization components). The horizontal axis is converted to z, with z_0 adjusted so that $z = 0$ corresponds to the input of FUT shown as the 1st peak in the spectrum. The 2nd peak at $z = 1.49\ m$ is caused by the reflection of a FC-APC connector between the circulator and SMF-28. The PSD suddenly increases at

$z = 17.73\ m$ which is the splicing point between SMF-28 and HSF, and the HSF has approximately 10dB higher scattering efficiency compared to SMF-28. The last peak at $z = 37.7\ m$ is the end of the HSF which is terminated with index matching gel. There are 4 traces in Fig.2 measured with 4 different settings of the PC located at $z = 24.1\ m$. Because the PC introduces negligible changes in attenuation, the 4 traces in Fig.2 are almost identical, and it is not possible to find the location of the PC. However, since the differential phase φ between E_x and E_y can be measured by the coherent receiver, it is possible to find the Stokes parameters defined as $s_1 = \left[|E_x|^2 - \left|E_y\right|^2\right]/S_0$; $s_2 = \left[2|E_x|\left|E_y\right| cos\,\varphi\right]/S_0$; $s_3 = \left[2|E_x|\left|E_y\right| sin\,\varphi\right]/S_0$. The SOP of the backscattered signal can be fully characterized as the function of z.

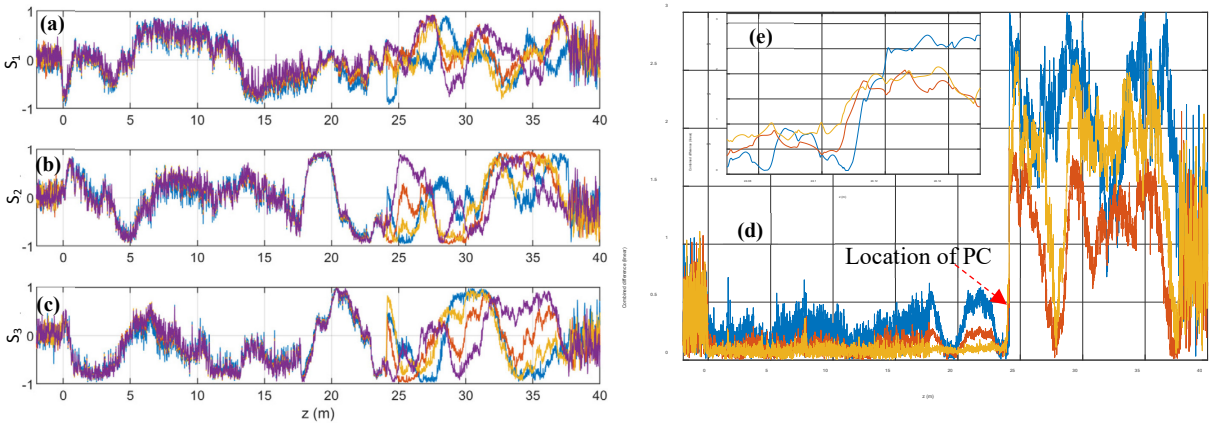

Fig 3. (a), (b), (c): $S_1(z)$, $S_2(z)$ and $S_3(z)$ for 4 different polarization controller settings (shown in different colors). (d) combined SOP change, (e) expanded view of combined SOP changes between different polarization settings

Fig 3 (a - c) show the measured $s_1(z)$, $s_2(z)$ and $s_3(z)$ for 4 different PC settings. In the section of SMF ($0 < z < 17.73\ m$), Rayleigh scattering is weak so that SNR is relatively poor. The HSF section ($17.73 < z < 37.7\ m$) has 10dB higher scattering which improves the SNR of the measured S-parameters in that region. The PC introduces abrupt SOP change at the location of $z = 24.1\ m$ which can be seen from the sudden changes in the Stokes parameters shown in Fig.3 (a-c). Comparing between S-parameters obtained with different PC settings, SOP changes for $z > 24.1\ m$ are uncorrelated as the optical signal passes twice (roundtrip) through the PC.

To have a single parameter to indicate the position where PC is applied, a combined SOP change can be used as $ds(z) = \sum_{n=1}^{3}\left|s_{n,A}(z) - s_{n,B}(z)\right|$, where $n = 1,2,3$ represent $s_1(z)$, $s_2(z)$ and $s_3(z)$, and $S_{n,A}(z), S_{n,B}(z)$ represent S parameters measured with two different PC settings (A and B). Fig 3(d) shows that there are sharp changes of combined SOP caused by the PC located at $z = 24.1\ m$. The inset of Fig 3(d) is an expanded view in the vicinity of $24.1\ m$ which indicates the PC is located at $z = 24.11 \pm 0.01\ m$. Note that the length of PC itself is $8\ mm$ which is part of the $\pm 10\ mm$ location uncertainty.

3. Conclusion

We demonstrated a simple measurement technique for distributed P-OFDR in which linear chirp is produced through digital modulation of an optical carrier, and the Stokes parameters of backscattered optical signal are measured in a coherent homodyne receiver. We demonstrated the ability to pinpoint the location of a PC with a spatial resolution on the order of $10\ mm$ with a chirping bandwidth of 26GHz. Phase continuity during frequency chirping ensures the measurement accuracy and continuity of Stokes parameters. Fully digital modulation also ensures excellent repeatability and high speed of measurements.

References

[1] P. Gysel and R. K. Staubli, *Journal of Lightwave Technology*, vol. 8, no. 4, pp. 561-567, April 1990.
[2] P. Westbrook, K. S. Feder and T. Kremp, " *2022 Optical Fiber Communications Conference and Exhibition (OFC)*, San Diego, CA, USA, 2022, pp. 01-03.
[3] T. Feng, J. Zhou, Yanling Shang, Xiaojun Chen, and X. Steve Yao, Opt. Express 28, 31253-31271 (2020).
[4] Z. Ding *et al*., *IEEE Sensors Journal*, vol. 23, no. 22, pp. 26925-26941, 15 Nov.15, 2023.
[5] S. Qu, Z. Wang, Z. Qin, Y. Xu, Z. Cong and Z. Liu, *IEEE Internet of Things Journal*, vol. 9, no. 4, pp. 2882-2889, 15 Feb.15, 2022.
[6] Changjiang Wei, Hongxin Chen, Xiaojun Chen, David Chen, Zhihong Li, and X. Steve Yao, Opt. Lett. 41, 2819-2822 (2016).
[7] Luca Palmieri, Andrea Galtarossa, and Tommy Geisler, Opt. Lett. 35, 2481-2483 (2010).
[8] H. Dong, P. Shum, M. Yan, J. Q. Zhou, G. X. Ning, Y. D. Gong, and C. Q. Wu, Opt. Express 14, 5067-5072 (2006).
[9] Ting Feng, Yanling Shang, Xichen Wang, Shengbao Wu, Anton Khomenko, Xiaojun Chen, and X. Steve Yao, Opt. Express 26, 25989-26002 (2018).
[10] Fiber-optic Measurement Techniques, R. Hui and M. Osullivan, Academic Press 2019.